Spectroscopy and anomalous emission of Ce doped elpasolite $Cs_2LiY Cl_6$

2004 J. Phys.: Condens. Matter 16 1887

(http://iopscience.iop.org/0953-8984/16/10/019)

INSTITUTE OF PHYSICS PUBLISHING JOURNAL OF PHYSICS: CONDENSED MATTER

J. Phys.: Condens. Matter **16** (2004) 1887–1897 PII: S0953-8984(04)73688-7

Spectroscopy and anomalous emission of Ce doped elpasolite Cs_2LiYCl_6

A Bessière[1], P Dorenbos[1,4], C W E van Eijk[1], L Pidol[2], K W Krämer[3] and H U Güdel[3]

[1] Radiation Technology Group, Interfaculty Reactor Institute, Delft University of Technology, Mekelweg 15, 2629 JB Delft, The Netherlands
[2] LCAES, UMR 7574, ENSCP 11 Rue P&M Curie, 75231, Paris Cedex 05, France
[3] Department of Chemistry and Biochemistry, University of Bern, Freiestrasse 3, 3000 Bern 9, Switzerland

E-mail: dorenbos@iri.tudelft.nl

Received 17 December 2003
Published 27 February 2004
Online at stacks.iop.org/JPhysCM/16/1887 (DOI: 10.1088/0953-8984/16/10/019)

Abstract

A 10 ns fast luminescence was observed at 270 nm in Cs_2LiYCl_6:Ce^{3+} in addition to the $5d_t$–4f Ce^{3+} doublet emission at 370 and 405 nm. This anomalous luminescence occurs exclusively for an excitation of the 4f–$5d_e$ transitions of Ce^{3+} around 210 nm. It is not excited under across band gap excitation which makes it an uncommon phenomenon. The emission shows a large Stokes shift of 1.2 eV that must be related to an excited state with a very strong electron–lattice interaction or possible involvement of conduction band states. The 270 nm emission undergoes thermal quenching between 140 and 250 K while the $5d_t$–4f Ce^{3+} emission gains intensity. The shape of the decay time spectra of the $5d_t$–4f Ce^{3+} emission reflects a temperature activated transfer from the anomalous state to the $5d_t$ lowest Ce^{3+} level.

1. Introduction

Cerium doped elpasolite compounds such as Cs_2LiYCl_6:Ce are of interest because the Ce^{3+} ions occupy a highly symmetrical site with a perfect octahedral point symmetry [1]. The 5d levels split into a lower triplet $5d_t$ state and an upper doublet $5d_e$ state separated by about 2.5 eV. This makes the level structure of Ce^{3+} relatively simple [2–4]. The pure and Ce doped compounds show fast (2 ns) decay time core–valence luminescence when excited by 14 eV photons [5]. Finally Cs_2LiYCl_6:0.1% Ce is an excellent thermal neutron scintillator with a very high light yield and a pulse shape that depends on the type of radiation used (γ-radiation or thermal neutrons) [6].

[4] Author to whom any correspondence should be addressed.

In the present paper an additional peculiar feature is discussed. As for Cs_3LuCl_6:Ce where the phenomenon was observed for the first time [7], a faster emission than the Ce $5d_t$–4f luminescence is detected at 270 nm when and only when the 4f–$5d_e$ transition of Ce is excited. This new type of emission starts to quench thermally above 120 K. The study of this quenching behaviour as well as a study of the decay time of the normal CE $5d_t$–4f emission with temperature enabled us to go further in the elucidation of the origin of anomalous emission in Cs_2LiYCl_6:Ce.

2. Experimental details

Single crystals of Cs_2LiYCl_6 doped with 0.1% and 3% Ce^{3+} were grown by the vertical Bridgman technique. Cs_2LiYCl_6 has a cubic elpasolite structure and crystallizes in the space group $Fm\bar{3}m$ with lattice parameter $a = 1048.57$ pm [1]. The crystals are hygroscopic. Emission, excitation and decay time spectra taken with synchrotron radiation were obtained for the bare crystals in vacuum. Decay time spectra under laser excitation were obtained for a crystal sealed in a small quartz ampoule.

Time-resolved excitation and emission spectra were recorded using synchrotron radiation at the SUPERLUMI station of the Synchrotron Strahlungslabor (HASYLAB) at the Deutsches Elektronen Synchrotron (DESY) in Hamburg, Germany. All excitation spectra were measured with 0.3 nm resolution of the excitation monochromator. The excitation spectra were corrected for the intensity of the excitation light by means of comparison with the excitation spectrum of Na salicylate. For recording the emission, a monochromator with a 300 grooves nm^{-1} grating blazed at 300 nm was used. The entrance and exit slit widths were chosen such as to optimize signal intensity without degrading wavelength resolution too much. Since emission bands are usually rather broad, wavelength resolution between 5 and 10 nm was often acceptable.

Three types of emission/excitation spectrum were recorded, denoted as 'fast', 'slow' and 'integral' in figures 1 and 2. The fast spectra correspond to light monitoring over a time window 5 ns wide and starting immediately after the excitation synchrotron pulse. For the slow spectra, emitted light is monitored over an 82 ns wide window starting after 89 ns delay. Integral spectra comprise all emitted light.

Lifetime measurements, after 355 nm laser excitation, were carried out using a fast digital oscilloscope. The third harmonic of an $Y_3Al_5O_{12}$:Nd laser was used as the excitation source.

3. Results

3.1. Excitation and emission spectra

Optical emission spectra of Cs_2LiYCl_6:0.1% Ce recorded at 10 K and room temperature (RT) for two distinct ultra-violet (UV) excitation ranges, respectively 210–216 and 180–185 nm, are shown in figure 1. At RT, exciting the crystal at 185 nm (figure 1(a)) leads to a spectrum composed of two intense bands peaking at 405 nm (3.06 eV) and 370 nm (3.35 eV). They are caused by transitions from the lowest 5d excited state ($5d_t$) to the two spin–orbit split ^2F states of Ce^{3+}. Furthermore, there is a slow and broadband luminescence at around 310 nm attributed to self-trapped exciton (STE) emission [2]. The spectrum is very similar to what is obtained under x-ray excitation [2, 5]. When excited at 216 nm the crystal exhibits again the Ce^{3+} doublet emission but does not show any STE luminescence (see figure 1(b)). At 10 K the emission spectrum at 180 nm excitation (see figure 1(c)) is almost identical to the one at RT at 185 nm excitation. The STE luminescence is just slightly less intense. However, at 10 K and 210 nm excitation a new feature appears in the spectrum (see figure 1(d)). In addition to

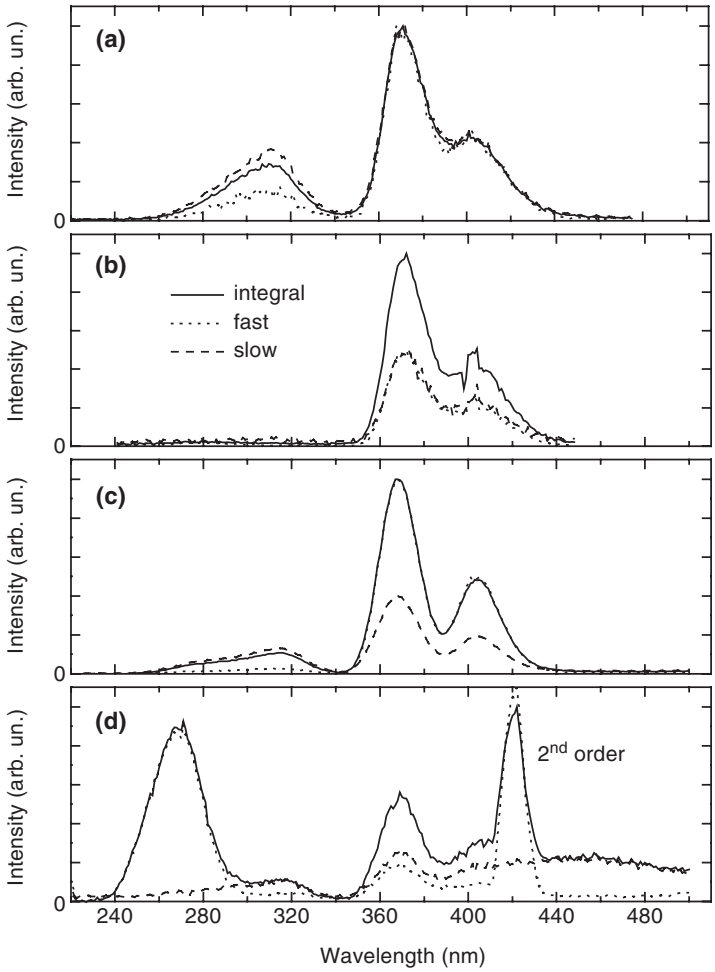

Figure 1. Emission spectra of Cs_2LiYCl_6:0.1% Ce excited at 185 nm at RT (a), at 216 nm at RT (b), at 180 nm at 10 K (c) and at 210 nm at 10 K (d). Each spectrum has its own arbitrary scale. The 'fast', 'slow' and 'integral' spectra were normalized to each other in order to demonstrate best the different contributions.

the fast emission due to the 5d–4f transitions of Ce^{3+} a fast and intense luminescence named 'anomalous' peaks at 270 nm. Its full width at half-maximum (FWHM) is 0.49 eV.

Figure 2 displays RT and 10 K optical excitation spectra monitoring either the Ce $5d_t$–4f emission at 370 nm or the anomalous luminescence at 270 nm. In figure 2(a) the excitation spectrum of d–f emission at RT is characterized by an intense band at around 335 nm and a double band at 210 and 216 nm yielding mainly fast luminescence. Secondly, a broad unstructured band below 194 nm is responsible for a slow emission process. It was shown elsewhere [5] that excitation by high energy radiation led to slow Ce 5d–4f emission due to energy transfer from STEs to Ce^{3+} centres. The band below 194 nm is therefore attributed to STE excitation. The band peaking around 335 nm is identified as the energy of transition from the 4f to the triplet $5d_t$ levels of Ce. The band falls partly beyond the instrumental limits and the spin–orbit splitting of the $5d_t$ state cannot be seen. The double band at 210 and 216 nm is related to direct excitation from the 4f ground state to the $5d_e$ levels of Ce. The 0.16 eV splitting

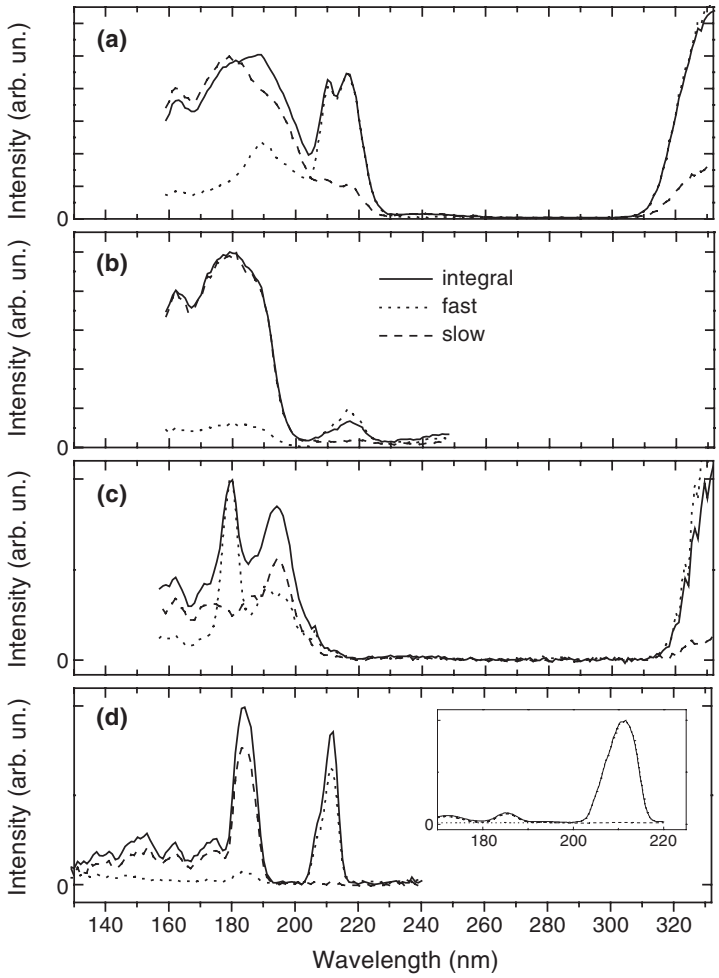

Figure 2. Excitation spectra of Cs_2LiYCl_6:0.1% Ce monitoring the 370 nm emission at RT (a), the 270 nm emission at RT (b), the 370 nm emission at 10 K (c) and the 270 nm emission at 10 K (d). Inset in (d): excitation spectra of Cs_2LiYCl_6:3% Ce monitoring the 270 nm emission at 10 K. Each spectrum has its own arbitrary scale. The 'fast', 'slow' and 'integral' spectra were normalized to each other in order to demonstrate best the different contributions.

between the two e_g levels cannot be caused by spin–orbit coupling because it transforms as U' in the double group of O_h. A Jahn–Teller coupling in this ^2E_g state, on the other hand, is possible and probable. The excitation bands at 216 and 210 nm will be respectively called $4f \rightarrow 5d_{e1}$ and $4f \rightarrow 5d_{e2}$ ones.

The spectrum in figure 2(b) monitoring the anomalous emission at 270 nm at RT is dominated by excitation bands of the STE emission. The STE emission peaks around 325 nm with a tail extending beyond 270 nm [2]. A remnant of this emission can be seen in figure 1(a). In addition to STE excitation, figure 2(b) reveals a weak double band between 205 and 225 nm corresponding to a fast emission process and similar to the double band observed in figure 2(a). The anomalous emission is therefore excited via the $4f–5d_e$ transitions at room temperature.

When the temperature is lowered to 10 K the $4f–5d_t$ transition is still present in the excitation spectrum of the $5d_t–4f$ Ce emission (see figure 2(c)) whereas the $4f–5d_e$ transitions

are not observed any longer. The slow spectrum shows a peak at 194 nm (6.4 eV) which is assigned to some kind of near defect exciton (NDE1) that slowly transfers the excitation energy to Ce^{3+} centres. NDEs are excitons created in the near vicinity of an impurity. The NDE1 peak overlaps with a broad and less intense band that continues towards shorter wavelength. The fast spectrum exhibits a second peak at 180 nm (6.9 eV) which we again attribute to the creation of near defect excitons (NDE2), but now in the vicinity of Ce^{3+}. A very fast transfer from NDEs to Ce^{3+} centres takes place and the decay time is the same as under direct excitation of the $5d_t$.

On the short wavelength side an excitation band around 175 nm is attributed to the creation of free excitons that slowly transfer their energy to CE centres. In pure Cs_2LiYC_6 an excitation peak was observed at the same wavelength [5]. The dip situated at wavelengths immediately below, i.e., around 166 nm in figures 2(a)–(d), is assigned to creation of free electrons at the bottom of the conduction band. On the basis of these assignments and previous results we estimate the bottom of the conduction band to be at $E_{VC} = 7.5$ eV, the maximum of the exciton band of the pure host to be at $E_{ex} = 7.0$ eV and the onset of the fundamental absorption to be at around $E_{fa} = 6.6$ eV.

The excitation spectrum of the anomalous emission at 10 K (see figure 2(d)) shows a fast non-symmetric band which may be viewed as a non-resolved double band peaking at 206 and 211.5 nm. The 211.5 nm band is dominant. The anomalous emission has a Stokes shift of about 1.2 eV. In addition a slow band is situated around 183 nm but it is likely to be related again to some sort of NDE with an emission that overlaps with the anomalous emission at 270 nm. This is evidenced in the inset of figure 2(d) that pertains to a 3% CE doped compound. At this concentration no STE emission is observed at 10 K and also the 183 nm band is almost absent in the excitation spectrum. Other excitation bands yielding the fast emission at 270 nm were not observed. In particular, across band gap excitation does not lead to the anomalous emission. The fast anomalous emission is therefore clearly and only based on the excitation of the $4f–5d_e$ transition of CE.

3.2. Temperature evolution

A single exponentially decaying emission is observed in the 10–840 K temperature range when the $4f–5d_t$ transition in Cs_2LiYCl_6:0.1% Ce is excited by a 355 nm laser. The decay times are shown as a function of temperature in figure 3. A 15 ns increase of the decay time with temperature is observed. Such an increase is similar to what is observed for many other Ce^{3+} doped compounds [8]. Quenching of the Ce^{3+} emission is not observed up to the instrumental temperature limit at 840 K. Clearly the $5d_t$ emitting state is very stable. The high quenching temperature indicates that the $5d_t$ electron–lattice interaction is small, which is also related to the relatively small Stokes shift of 0.2 eV. Furthermore, luminescence quenching by means of auto-ionization of the $5d_t$ electron to conduction band states is improbably suggesting that the $5d_t$ state is well below (>1 eV) the bottom of the conduction band.

Excitation spectra of the anomalous emission were recorded at temperatures between 10 and 270 K for Cs_2LiYCl_6:3% Ce. With temperature increase, the wavelength of maximum intensity of the $5d_e$ related band $\lambda_m(T)$ drifts slightly, from 211.5 to 216 nm; see figure 2(d) and 2(a). Emission spectra, as well as decay time spectra for 270 and 370 nm emissions, were recorded for an excitation $\lambda_m(T)$ at several temperatures. The light yields for both Ce $5d_t–4f$ luminescence and anomalous emission are shown in figure 4 as a function of temperature. From 100 to 250 K an anti-correlated evolution is observed. The Ce emission gains intensity whereas the anomalous emission is decreasing.

The anomalous emission shows a mono-exponential decay with a characteristic decay time of 9.8 ns at 10 K. This is 2.5 times faster than that of the normal Ce^{3+} emission and can be

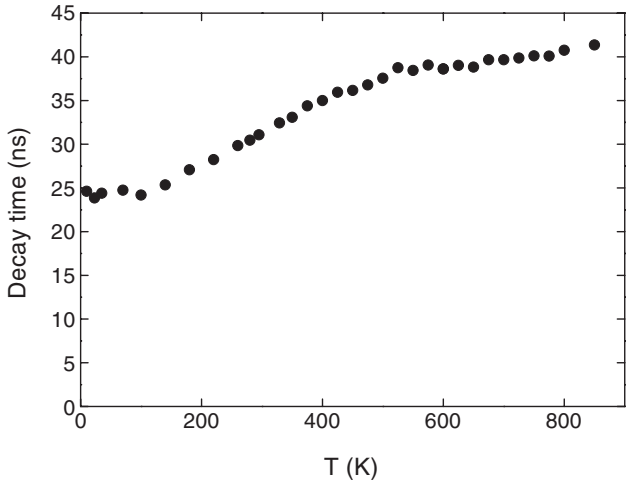

Figure 3. Decay times as a function of temperature for the 370 nm emission of Cs_2LiYCl_6:0.1% Ce excited at 355 nm.

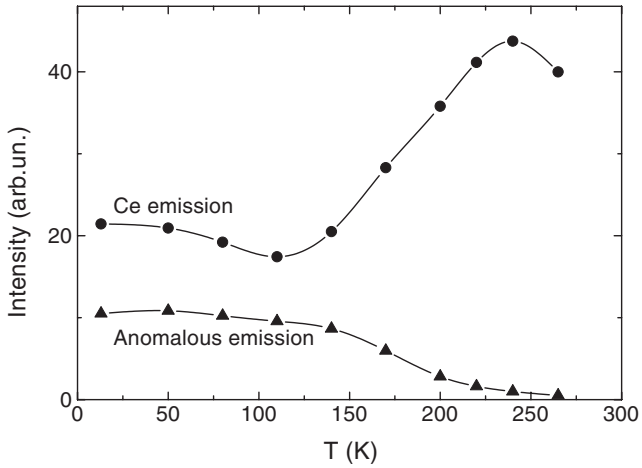

Figure 4. Integral luminescence intensities of the uncorrected emission spectra as a function of temperature for the $5d_t$–4f Ce^{3+} emission and the anomalous emission of Cs_2LiYCl_6:3% Ce, both excited at the maximum of the 4f–$5d_e$ absorption band. This maximum shifts from 211.5 to 216 nm with temperature increase.

attributed to the λ^3 dependence of the decay time on the emission wavelength. The temperature dependence of the decay time is shown in figure 5. It exhibits the same type of quenching behaviour as the light yield in figure 4. The solid curve through the data in figure 5 represents a model calculation used to describe thermal quenching of luminescence. The decay time is given by

$$\tau(T) = \frac{\frac{1}{\Gamma_\nu}}{1 + \frac{\Gamma_0}{\Gamma_\nu} \exp\left(-\frac{\Delta E_q}{kT}\right)} \tag{1}$$

where Γ_0 and Γ_ν are respectively the thermal quenching rate at $T = \infty$ and the radiative transition rate of the anomalous state. ΔE_q is the activation energy for thermal quenching and

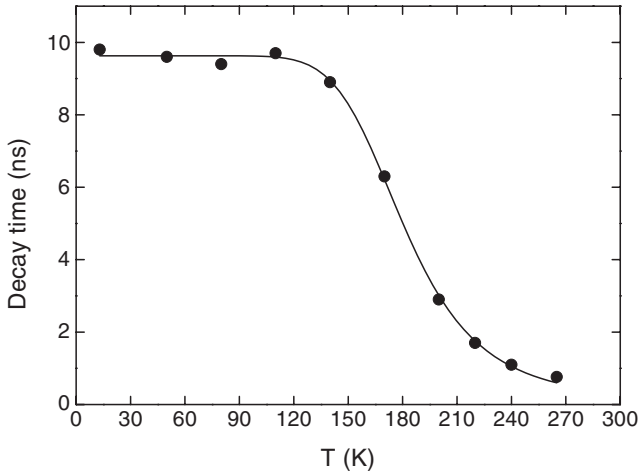

Figure 5. Decay time as a function of temperature for the anomalous emission at 270 nm of Cs_2LiYCl_6:3% Ce under 4f–$5d_e$ excitation. The full curve is from a model calculation.

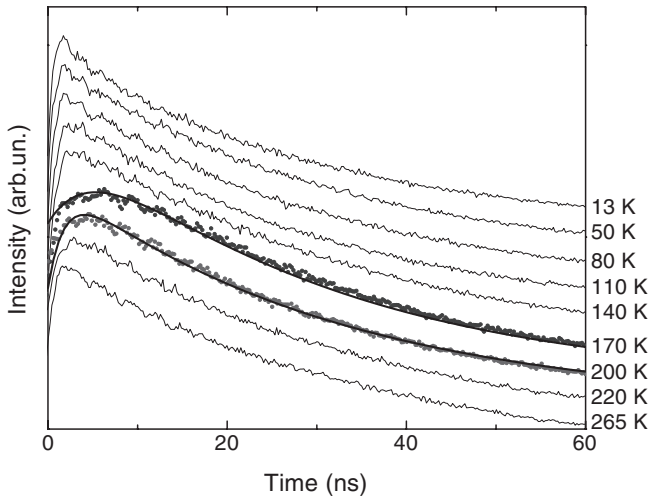

Figure 6. Decay time spectra on a semi-log scale for the 370 nm emission of Cs_2LiYCl_6:3% Ce excited in the $5d_e$ level for various temperatures. The full curves represent, for 170 and 200 K, modelling curves.

k the Boltzmann constant. From a fit with equation (1), the values $\Gamma_0 = 5.8 \times 10^{11}$ Hz and $\Delta E_q = 0.14$ eV are obtained.

The decay time spectra of Ce emission in Cs_2LiYCl_6:3% Ce for temperatures between 13 and 265 K are displayed in figure 6. Their shapes evolve with temperature. For temperatures situated on the plateaus of the curve in figure 5, i.e., between 10 and 110 K and beyond 265 K, the spectra in figure 6 are single exponential. When the anomalous emission is being quenched, i.e., for temperatures between 140 and 240 K, the $5d_t$–4f Ce emission is delayed by several nanoseconds which leads to a distinct rise time in the decay time spectra. Such a rise time indicates that the Ce emitting $5d_t$ state is populated via a transfer process. The timescale of the transfer is of the same order as the quenching rate of the anomalous emission.

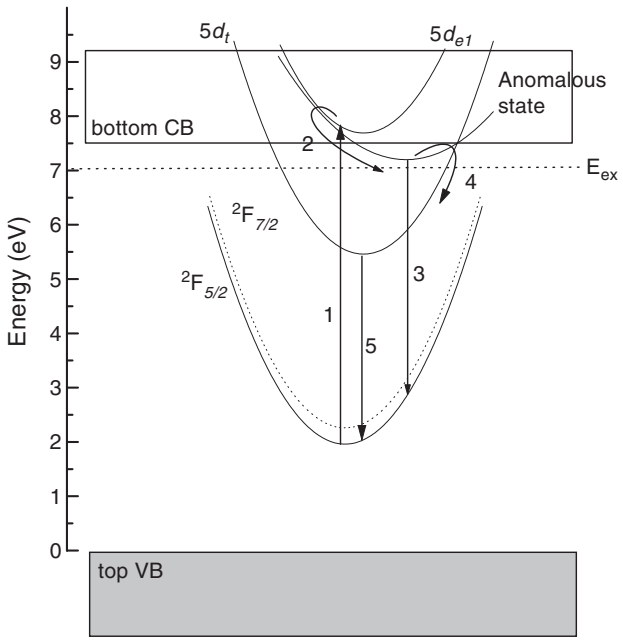

Figure 7. The scheme of Ce^{3+} energy levels in the host matrix Cs_2LiYCl_6. The Ce^{3+} levels are illustrated with a configuration coordinate (CC) diagram. The energy of the bottom of the conduction band and the top of the valence band are shown. (For these levels there is no physical meaning for the *x*-axis.)

4. Discussion and conclusions

The excitation spectra provide the energy differences between the different Ce^{3+} levels within the Cs_2LiYCl_6 matrix, and also between the top of the valence and the bottom of the conduction band of the host Cs_2LiYCl_6. The energy differences between the 4f ground state and $5d_t$, $5d_{e1}$ and $5d_{e2}$ are respectively 3.5, 5.7 and 5.9 eV. They were used for constructing the scheme in figure 7.

Suppose that the $5d_e$ levels are situated below the bottom of the conduction band; then the anomalous emission may be due to a direct transition from the $5d_e$ back to the $^2F_{7/2}$ and $^2F_{5/2}$ states. Such emission was suggested by Kato *et al* for $CaGa_2S_4$:Ce [9] and by Tanner *et al* [4] for $Cs_2NaErCl_6$:Ce^{3+}. However, with a $5d_e$ level located inside the forbidden gap we do not have an explanation for the very large Stokes shift of 1.2 eV that is six times larger than that of the normal 5d–4f emission. The width of the anomalous emission (FWHM = 0.49 eV) is of the same order as the total width (FWHM = 0.46) of the normal Ce^{3+} emission between 360 and 415 nm, whereas considering the large Stokes shift much wider band emission would be expected. More importantly, we cannot explain the absence of the anomalous emission when exciting across the band gap of the host crystal. We therefore propose a different mechanism that is based on $5d_e$ levels positioned inside the conduction band. Energy levels located at the bottom of the conduction band then participate in the emitting state of the anomalous emission as was also proposed by Dorenbos *et al* for the anomalous emission in Cs_3LuCl_6:Ce [7]. After excitation of an electron from the 4f to a $5d_e$ level represented by arrow 1 in figure 7, a non-radiative relaxation, shown as arrow 2, occurs where the electron reaches a state, called the anomalous state, constituted of a mix between states from the bottom of the conduction

Table 1. Values of Γ_d, Γ_a and Γ_t used for fitting the decay time spectra in figure 6. $N_a(0)/N_d(0)$ was obtained after simulation.

T	Γ_d (10^8 Hz)	Γ_a^{tot} (10^8 Hz)	Γ_t (10^8 Hz)	$N_a(0)/N_d(0)$
140	0.34	1.12	0.10	—
170	0.33	1.59	0.57	2.18
200	0.32	3.33	2.31	2.18

band and $5d_e$ levels. Physically this implies that the $5d_e$ electron is partly ionized from Ce but remains localized around Ce. The anomalous emission symbolized by arrow 3 in figure 7 then originates from the recombination of an electron in this state with the hole left behind on the Ce. The situation is quite similar to the anomalous emission occasionally observed for Eu^{2+} and Yb^{2+} doped compounds [10].

The thermal quenching of the anomalous emission in relation to the increase of the $5d_t$–4f luminescence intensity between 140 and 240 K in figure 4 is interpreted as a temperature activated transfer from the anomalous state to the $5d_t$ lowest emitting state schematized by arrow 4. The activation energy of 0.14 eV calculated for this process is viewed as the energy difference between the bottom of the anomalous state and the crossing point with the parabola belonging to the $5d_t$ state in the configuration coordinate diagram of figure 7. The resulting $5d_t$–4f emission is symbolized by arrow 5.

If we consider that the number $N_a(t)$ of populated anomalous states has a rate $\Gamma_a(T)$ for decreasing radiatively by anomalous emission and a rate $\Gamma_t(T)$ for decreasing by transfer to the $5d_t$ state because of thermal activation, the change in $N_a(t)$ is given by

$$\frac{dN_a(t)}{dt} = -\Gamma_a(T)N_a(t) - \Gamma_t(T)N_a(t) \tag{2}$$

where $N_d(t)$ is the number of populated $5d_t$ states with a rate $\Gamma_d(T)$ for decreasing by radiative transitions to the 4f ground state. $N_d(t)$ increases due to the transfer from the anomalous state. The change in $N_d(t)$ is given by

$$\frac{dN_d(t)}{dt} = -\Gamma_d(T)N_d(t) + \Gamma_t(T)N_a(t). \tag{3}$$

Solving both equations for $N_a(t)$ and $N_d(t)$ gives

$$N_a(t) = N_a(0)e^{-(\Gamma_a(T)+\Gamma_t(T))t} \tag{4}$$

and

$$N_d(t) = \left(N_d(0) + \frac{\Gamma_t(T)N_a(0)}{\Gamma_a(T)+\Gamma_t(T)-\Gamma_d(T)}\right)e^{-\Gamma_d(T)t} - \frac{\Gamma_t(T)N_a(0)}{\Gamma_a(T)+\Gamma_t(T)-\Gamma_d(T)}e^{-(\Gamma_a(T)+\Gamma_t(T))t} \tag{5}$$

with $N_a(0)$ and $N_d(0)$ the initial populations of the anomalous and the $5d_t$ state at $t = 0$.

The constant value of 9.8 ns for the decay time of the anomalous emission between 10 and 120 K in figure 5 indicates that for the temperatures of interest the radiative transition rate does not depend on temperature. The total decay rate for the anomalous emission is then given by

$$\Gamma_a^{tot}(T) = 1.02 \times 10^8 + \Gamma_t(T) \text{ Hz}. \tag{6}$$

Values for $\Gamma_a^{tot}(T)$, $\Gamma_d(T)$ and $\Gamma_t(T)$ at 140, 170 and 200 K obtained from figures 5, 3 and equation (6) are compiled in table 1.

Decay time spectra for the $5d_t$–4f Ce emission excited by the 4f–$5d_{e1}$ transition are shown in figure 6. At 13 K, $\Gamma_t = 0$ and equation (5) reduces to a single-exponential decay of the $N_d(0)$ populated $5d_t$ state. At 265 K, Γ_t is very large and equation (5) reduces again to a single-exponential decay but now with an increased number of $N_d(0) + N_a(0)$ populated $5d_t$ states. Both situations agree with figure 6 and with the evolution of luminescence intensity in figure 4.

Results from model simulations for $T = 170$ and 200 K using equation (5) are represented by the solid curves through the data in figure 6. The values of Γ_d, Γ_a^{tot}, Γ_t in table 1 are from experimental data and the ratio $N_a(0)/N_d(0)$ is the only free parameter. The model enables a good simulation of the decay time spectra at $T = 200$ and 170 K by using a ratio of 2.18 at both temperatures. At 140 K the transfer speed for the 100 ns rate is much slower than the anomalous decay rate and the decay curve is already nearly single exponential. Some processes not considered in the rate equations (2) and (3), such as thermal quenching of the anomalous state by auto-ionization or by multi-phonon relaxation or initial populations $N_d(0)$ and $N_a(0)$ that depend on temperature, may be involved, leading to difficulties in accurately reproducing the decay curves in figure 6. Furthermore, the decay curves should be deconvoluted from the time resolution of the detection system and the pulse shape of the exciting synchrotron pulse. Nevertheless, equation (5) already provides a good qualitative description of the anomalous and normal emission intensity as a function of time and temperature that is consistent with the model sketched in figure 7.

It was considered in [7] that the transition responsible for the anomalous emission is a type of dipole allowed charge transfer involving conduction band states that is different in nature to the well-known $5d_t$–4f transition. The involvement of the conduction band provides a lowering of the energy which then explains the high value found for the Stokes shift without introducing exceptional broadening of the anomalous emission band. Note that the 0.49 eV FWHM of the anomalous emission is of the same magnitude as the total width of the Ce^{3+} doublet emission to the $^2F_{5/2}$ and $^2F_{7/2}$ final states.

In presenting the results of figure 2 we noticed that anomalous emission is more efficiently excited in the $5d_{e1}$ state than in the $5d_{e2}$ states whereas this is not the case for the $5d_t$–4f Ce emission. An efficient absorption band at around 203 nm may compete with the excitation of the anomalous emission. Actually, a strong absorption band was observed by van Loef *et al* [5] for pure Cs_2LiYCl_6 at this energy, but this point needs to be further elucidated.

So far two other compounds have been found that exhibit a similar anomalous emission. Cs_3LuCl_6:Ce shows an emission at 281 nm with a 10.5 ns single-exponential decay and a highly selective excitation region between 202 and 211 nm [7]. The results are very similar to those for Cs_2LiYCl_6:Ce. Also, in the two compounds the surroundings of Ce^{3+} are quite similar. It was suggested that a large energy gap between the lowest $5d_e$ state and the highest $5d_t$ state (2.43 eV) together with small maximum phonon efficiency are the key factors that prevent a fast multi-phonon relaxation from the $5d_e$ state to the $5d_t$ states. Instead the system relaxes to the anomalous state. Cs_2LiYCl_6:Ce has a very similar energy difference between the lowest $5d_e$ state and the highest $5d_t$ state (2.5 eV) and presumably has a similar maximum phonon frequency to Cs_3LuCl_6:Ce.

The situation is slightly different for the second example observed up to now. In $CaGa_2S_4$:Ce the energy difference between the lowest 5d state and the highest one is only 0.92 eV but the maximum phonon efficiency of the sulfide may also be significantly smaller than for the two chloride compounds.

We anticipate that most cubic chloride elpasolites will reveal anomalous emission. To obtain conclusive evidence on the true nature of the emitting state, the location of the Ce^{3+} energy levels relative to the host bands should be determined. With x-ray photoelectron

spectroscopy and photoconductivity measurements we expect to gain further insight into the mechanism of anomalous emission.

Acknowledgments

This work was supported by the Dutch Technology Foundation (STW) and by the IHP-Contract HPRI-CT-1999-00040 of the European Commission. The authors thank Dr M Kirm for his assistance in the SUPERLUMI experiments at the HASYLAB of DESY, Hamburg, and P Aschehoug for his technical support in laser excitation at the LCAES, ENSCP, Paris.

References

[1] Reber C, Güdel H U, Meyer G, Schleid T and Daul C A 1989 *Inorg. Chem.* **28** 3249
[2] Combes C M, Dorenbos P, van Eijk C W E, Krämer K W and Güdel H U 1999 *J. Lumin.* **82** 299
[3] Schwartz R W and Schatz P N 1973 *Phys. Rev.* B **8** 3229
[4] Tanner P A, Mak C S K, Edelstein N M, Murdoch K M, Liu G, Huang J, Seijo L and Barandiaran Z 2003 *J. Am. Chem. Soc.* **125** 13225
[5] van Loef E V D, Dorenbos P, van Eijk C W E, Krämer K W and Güdel H U 2002 *J. Phys.: Condens. Matter* **14** 1
[6] Bessière A, Dorenbos P, van Eijk C W E, Krämer K W and Güdel H U 2004 *Nucl. Instrum. Methods* A at press
[7] Dorenbos P, van Loef E V D, van Eijk C W E, Krämer K W and Güdel H U 2003 *Phys. Rev.* B **68** 125108
[8] Lyu L-J and Hamilton D S 1991 *J. Lumin.* **48/49** 251
[9] Kato A, Yamazaki M, Najafov H, Iwai K, Bayramov A, Hidaka C, Takizawa T and Iida S 2003 *J. Phys. Chem. Solids* **64** 1511
[10] Dorenbos P 2003 *J. Phys.: Condens. Matter* **15** 2645